Carcinogenesis vol.32 no.10 pp.1525–1532, 2011
doi:10.1093/carcin/bgr171
Advance Access publication July 27, 2011

(-)-Epigallocatechin-3-gallate and DZNep reduce polycomb protein level via a proteasome-dependent mechanism in skin cancer cells

Subhasree Roy Choudhury[1], Sivaprakasam Balasubramanian[1], Yap Ching Chew[1], Bingshe Han[1], Victor E.Marquez[3] and Richard L.Eckert[1,2,4,*]

[1]Department of Biochemistry and Molecular Biology and [2]Department of Dermatology, University of Maryland School of Medicine, Baltimore, MD 21201, USA, [3]Laboratory for Medicinal Chemistry, Center for Cancer Research, National Cancer Institute, Frederick, MD 21702, USA and [4]Department of Obstetrics, Gynecology and Reproductive Sciences, University of Maryland School of Medicine, Baltimore, MD 21201, USA

*To whom correspondence should be addressed. Department of Biochemistry and Molecular Biology, University of Maryland School of Medicine, 108 North Greene Street, Room 103, Baltimore, MD 21201, USA. Tel: +1 410 706 3220; Fax: +1 410 706 8297;
Email: reckert@umaryland.edu

Polycomb group (PcG) protein-dependent histone methylation and ubiquitination drives chromatin compaction leading to reduced tumor suppressor expression and increased cancer cell survival. Green tea polyphenols and *S*-adenosylhomocysteine (AdoHcy) hydrolase inhibitors are important candidate chemopreventive agents. Previous studies indicate that (-)-epigallocatechin-3-gallate (EGCG), a potent green tea polyphenol, suppresses PcG protein level and skin cancer cell survival. Inhibition of AdoHcy hydrolase with 3-deazaneplanocin A (DZNep) inhibits methyltransferases by reducing methyl group availability. In the present study, we examine the impact of EGCG and DZNep cotreatment on skin cancer cell function. EGCG and DZNep, independently and in combination, reduce the level of PcG proteins including Ezh2, eed, Suz12, Mel18 and Bmi-1. This is associated with reduced H3K27me3 and H2AK119ub formation, histone modifications associated with closed chromatin. Histone deacetylase 1 level is also reduced and acetylated H3 formation is increased. These changes are associated with increased tumor suppressor expression and reduced cell survival and are partially reversed by vector-mediated maintenance of Bmi-1 level. The reduction in PcG protein level is associated with increased ubiquitination and is reversed by proteasome inhibitors, suggesting proteasome-associated degradation.

Introduction

Polycomb group (PcG) proteins regulate genes involved in development, differentiation and survival via epigenetic (e.g. chromatin modification) mechanisms (1,2). This mechanism involves sequential action of two polycomb repressor complexes, PRC2 and PRC1. Ezh2, Suz12, eed and RBAP48 comprise four core proteins of the PRC2 complex. Ezh2, a methyltransferase, is the catalytic subunit of this complex and methylates lysine 27 of histone H3 to form histone H3 trimethylated on lysine 27 (H3K27me3) (3). Suz12, eed (embryonic ectoderm development) and RBAP48 (retinoblastoma-binding protein p48) are non-catalytic subunits that are required for optimal Ezh2 enzymatic activity. Ezh2 association with Suz12 and eed results in a 1000-fold increase in Ezh2 enzymatic activity (4,5). Alternate subunits can substitute including Ezh1 for Ezh2, RBAP46 for RBAP48, and there are several eed variants (6).

Abbreviations: AdoHcy, S-adenosylhomocysteine; cdk, cyclin-dependent kinase; DZNep, 3-deazaneplanocin A; EGCG, (-)-epigallocatechin-3-gallate; FITC, fluorescein isothiocyanate; H3Ac, acetylated histone H3; H3K27me3, histone H3 trimethylated on lysine 27; H2AK119ub, histone H2A ubiquitinated on lysine 119; MTT, 3-(4,5-dimethylthiazole-2-yl)-2,5-biphenyl tetrazolium bromide; PcG, polycomb group; PRC, polycomb repressorcomplex.

The core PRC1 complex includes Ring1B, Bmi-1, PH1 and CBX (6). The CBX protein binds to the H3K27me3-modified histone to anchor the PRC1 complex to chromatin (7). Ring1B, the catalytic subunit, is a histone ubiquitin ligase that catalyzes formation of histone H2A ubiquitinated on lysine 119 (H2AK119ub) (8) and Bmi-1 is necessary for optimal Ring1B activity (8). H2AK119 ubiquitination (H2Ak119ub) by Ring1B is a key step in the process leading to closed chromatin. Alternate partners in the PRC1 complex include Ring1 for Ring1B, MEL18 or NSPC1 for Bmi-1, CBX2, 6, 7 or 8 for CBX and PH2 for PH1 (1,6,9,10). Chromatin modification by PRC2 and PRC1 is a sequential process. PRC2 interaction with chromatin initiates the process. The PRC2 complex Ezh2 protein catalyzes H3K27me3 formation. Next, the PRC1 complex CBX protein binds to H3K27me3 to anchor the PRC1 complex to chromatin. Ring1B protein then catalyzes formation of H2AK119ub (11,12). The combined impact of PRC2/PRC1 action is establishing a closed chromatin state leading to a stable reduction of tumor suppressor expression (1,13).

We observe increased expression of PcG proteins in immortalized keratinocytes and skin cancer cell lines as compared with normal cells and tissue (14,15). This is associated with increased cell proliferation, suggesting that altered epigenetic regulation is likely to contribute to cancer development. We examined the impact of a green tea-derived bioactive polyphenol, (-)-epigallocatechin-3-gallate (EGCG), on expression and function of two key PcG proteins, Bmi-1 and Ezh2 (15). Green tea polyphenols are important diet-derived candidate chemopreventive agents (16–19). Treating epidermal squamous cell carcinoma cells with EGCG reduces Bmi-1 and Ezh2 level and cell survival. This is associated with a global reduction in histone H3K27me3 level, indicating that EGCG suppresses PRC2 complex function. This change is associated with reduced expression of cyclin-dependent kinase (cdk) 1, cdk2, cdk4, cyclin D1, cyclin E, cyclin A and cyclin B1 and increased expression of the cdk inhibitors, $p21^{Cip1}$ and $p27^{Kit1}$. Apoptosis is also enhanced including increased caspase 9, 8 and 3 and Poly (ADP-ribose) polymerase cleavage (15). Bax level is increased and Bcl-xL level is suppressed. Vector-mediated maintenance of Bmi-1 expression reverses the EGCG-dependent changes, suggesting that reduced PcG protein function is a key event (15,20).

The PRC2 complex protein, Ezh2, is a histone methyltransferase that catalyzes formation of H3K27me3 (9,21). We reasoned that reducing availability of donor methyl groups would reduce cell survival by reducing H3K27me3 formation. In the present study, we examine the impact of cotreating cells with EGCG and 3-deazaneplanocin A (DZNep). DZNep, a 3-deazaadenosine analog, is a potent inhibitor of *S*-adenosylhomocysteine (AdoHcy) hydrolase (22–25). Inhibiting AdoHcy hydrolase results in accumulation of AdoHcy, which leads to product inhibition of *S*-adenosyl-L-methionine-dependent methyltransferases (24). This indirectly inhibits methyltransferase activity by limiting available methyl donor groups (26). A variety of effects of these inhibitors have been described (26,27) and recent studies suggest that they suppress Ezh2 function (28). DZNep appears to be a unique chromatin-remodeling compound that can deplete cellular PRC2 protein level and reduce histone methylation (28–36). Our results show that both EGCG and DZNep reduce PcG protein level, suppress cell cycle progression and stimulate apoptosis and that combined treatment is more effective than each single agent. Additional studies reveal that these agents stimulate proteasome-dependent degradation of the PcG proteins, which can be inhibited by proteasome inhibitors.

Materials and methods

Chemicals, reagents and adenoviruses

DZNep was described previously (22,23) and EGCG was purchased from Sigma (St Louis, MO). DZNep and EGCG were dissolved, respectively, in water and dimethyl sulfoxide. The 3-(4,5-dimethylthiazole-2-yl)-2,5-biphenyl

tetrazolium bromide (MTT) cell viability assay was from Millipore Chemicon (Temecula, CA), and the annexin V-fluorescein isothiocyanate (FITC) apoptosis assay was from BD Biosciences (San Jose, CA). Mitochondrial membrane potential and caspase activity assay systems were from Cell Technology (Mountain View, CA). Ezh2 antibody was from BD Transduction Labs (San Jose, CA). Antibodies to Bmi-1 (ab14389) and eed (ab4469) were from Abcam (Cambridge, MA). Anti-Suz12 (04-046), anti-H3K27me3 (07-449) and anti-histone H3 trimethylated on lysine 9 (07-442) were from Upstate (Lake Placid, NY). Cyclin D1 (554180) and PARP (556494) antibodies were from BD Pharmingen (San diego, CA). Anti-cdk4 (sc-601), anti-GAPDH (sc-25778), anti-Proliferating cell nuclear antigen (sc-56), anti-ubiquitin (sc-9133), anti-Bax (sc-493), anti-IgG (sc-2025), anti-Mel18 (sc-10744) and anti-$p27^{kit1}$ (sc-1641) were from Santa Cruz Biotechnology Inc (Santa Cruz, CA). Antibodies to HDAC1 (#2062), caspases 3 (#9665) and $p21^{Cip1}$ (2947) were from Cell Signaling Technology (Danvers, MA). Antibodies to H2AK119ub (AB10029) and acetylated H3 (06-599) were from Millipore (Billerica, MA). Anti-caspase-3 (#9661) and anti-cleaved PARP (#9541) were from Cell Signaling Technology. Secondary antibodies included horseradish peroxidase-conjugated sheep anti-mouse IgG or horseradish peroxidase-conjugated donkey anti-rabbit IgG (GE healthcare, Buckinghamshire, UK). Lactacystin (L6785) and mouse anti-β-actin (A5441) were obtained from Sigma.

Cell proliferation and viability

SCC-13 and A431 cells were grown in Dulbecco's modified Eagle's medium supplemented with D-glucose, L-glutamine, 0.1 mg/ml sodium pyruvate, 100 U/ml penicillin, 100 U/ml streptomycin and 5% fetal bovine serum. Normal human keratinocytes were maintained in keratinocyte serum-free medium. For proliferation studies, cells were treated with 2.5 μM DZNep or 50 μM EGCG alone or in combination for 24 h and cell number was then counted. To measure cell viability, 1×10^4 cells were seeded into 96-well plates and allowed to attach overnight before exposure to DZNep (1, 2.5, 5 and 10 μM) or EGCG (5, 25, 50 and 100 μM) either alone or in combination for 24 h. Viability was assessed by MTT assay. For cell cycle analysis, SCC-13 cells were seeded at 1×10^5 cells per well into six-well plates, permitted to attach and treated with DZNep or EGCG alone or in combination for 24 h prior to harvest for cell cycle analysis (14).

Apoptosis

Annexin V-FITC-binding assay was used to detect apoptosis and necrosis. SCC-13 cells (1×10^5) were plated in 35 mm wells and after attachment treated with DZNep or EGCG for 24 h. Adherent cells were released with trypsin and combined with non-adherent cells prior to treatment with propidium iodide and annexin V-FITC and assay of propidium iodide content and annexin V-FITC by cell sorting.

Mitochondrial membrane potential and caspase activity assays

SCC-13 cells (1×10^5), in 35 mm wells, were treated with DZNep and or EGCG and after 24 h were stained with mitochondrial membrane potential cationic dye and caspase detection reagent (FAM-DEVD-FMK) at 37°C for 60 min. The cells harvested with trypsin and washed for analysis using a BD-LSR Flow Cytometer (BD Biosciences).

Immunological analysis

SCC-13 cells were treated for 24–48 h with the indicated treatment and harvested with trypsin for extract preparation. Extract was electrophoresed on 4–15% denaturing and reducing polyacrylamide gradient gels and transferred to nitrocellulose. The membrane was blocked with 20 mM Tris–HCl, pH 7.6 containing 0.1% Tween 20 and 5% powdered milk and then incubated with appropriate primary and secondary antibodies. Antibody binding was visualized using chemiluminescence detection reagent. For immunohistology, SCC-13 cells, growing on coverslips, were treated with DZNep or EGCG for 24 h. At the end of treatment, cells were incubated with 500 nM MitoTracker-Red CMXRos for 30 min at 37°C and then fixed with 4% paraformaldehyde and methanol permeabilized. The cells were then incubated overnight with primary antibody. After washing and incubation with secondary antibody, the cells were stained with Hoechest dye for 5 min and fluorescence was visualized using an Olympus OX81 spinning disc confocal microscope (×40 oil).

Detection of ubiquitinated PcG proteins

SCC-13 cells were treated with appropriate concentrations EGCG or DZNep in the absence or presence of 0.5 μm lactacystin for 24 h. Total cell extract (30 μg) was utilized for immunoblot detection of Ezh2, Bmi-1, H3K27me3 and ubiquitin. To detect specific ubiquitination of Bmi-1 and Ezh2, 75 μg of total extract was immunoprecipitated with anti-IgG, anti-Bmi-1 or anti-Ezh2 and the precipitate was electrophoresed for immunoblot with anti-ubiquitin.

Overexpression of Bmi-1 and challenge with DZNep and EGCG

SCC-13 cells (8×10^4 per well) were seeded in 35 mm wells and permitted to attach overnight. On day 0, the cells were infected with 2.5 Multiplicity of Infection of tAd5-EV or tAd5-hBmi-1 in the presence of 2.5 Multiplicity of Infection of Ad5-TA helper virus in Dulbecco's modified Eagle's medium without supplements for 3 h. After 3 h, supplementation was restored and at 24 h postinfection, the cells were treated with medium containing either dimethyl sulfoxide or DZNep (2.5 or 5 μM) or EGCG (50 or 100 μM) and incubation was continued for an additional 24 h. The cells were then harvested in 0.025% trypsin containing 1 mM ethylenediaminetetraacetic acid and cell number was counted using hemocytometer. Empty and Bmi-1 encoding adenoviruses were described previously (15,20).

Results

DZNep and EGCG treatment reduces SCC-13 cell viability

We first examined the impact of cotreatment with EGCG and DZNep on squamous cell carcinoma SCC-13 cell survival. Figure 1A shows that both agents reduce cell number as monitored by MTT assay and that combined treatment further reduces cell survival. Concentrations for cotreatment were selected as 2.5 μM DZNep and 50 μM EGCG (38). This combined action is reflected in a substantial additive reduction in cell number when cells are treated with 2.5 μM DZNep and 50 μM EGCG (Figure 1B). These agents also impact cell morphology. Figure 1C shows a distinctly different morphology in cells treated with DZNep versus EGCG. EGCG, in particular, causes formation of cells containing large blebs characteristic of apoptosis.

We next examined the impact of these agents on cell cycle. Figure 2A shows that treatment with DZNep reduces the percent of cells in G_1 and G_2 by a combined 27% and that these cells are shifted to S phase. In contrast, EGCG produces only a slight change in distribution. Remarkably, treatment with DZNep + EGCG results in an absence of G_2 phase cells. As shown in Figure 2B, both DZNep and EGCG reduce cdk4 and cyclin D1 level, and treatment with both agents produces further suppression. These treatments also reduce the level of the proliferation marker, proliferating cell nuclear antigen. In contrast, the level of the G_1 cdk inhibitors, $p21^{Cip1}$ and $p27^{Kip1}$, is increased.

DZNep and EGCG enhance apoptosis

These initial studies suggested a modest increase in the number of $subG_1$ cells (Figure 2A). To confirm that these agents cause apoptosis, we treated with twice the amount of each agent and in combination. This treatment caused a marked increase in the number of $subG_1$ events in EGCG- and DZNep-treated cells and this effect is greater in cells treated with both agents (Figure 2C). To explore the basis of this response, we monitored the effect on apoptosis status by monitoring annexin V distribution. Figure 3A shows a slight increase in the percent early-apoptotic events (lower right quadrant) after DZNep or EGCG treatment and an additional increase when both agents are present. Figure 3B shows an increase in the number of cells with reduced mitochondrial membrane potential (lower left quadrant) and an increase in caspase 3/7 activity (lower right quadrant). The largest increase in caspase activity is observed for combined treatment with both agents. To understand the molecular mechanism underlying these responses, we measured changes in apoptotic effectors. We observe a marked increase in Bax conversion to the lower mass proapoptotic form, reduced procaspase-3 level and increased PARP cleavage (Figure 3C). Some endpoints are more responsive to EGCG and others to DZNep. We next assessed Bax subcellular location. Mitochondria were stained with MitoTracker (red) and then fixed and stained with anti-bax (green). As shown in Figure 3D, the combined treatment with EGCG and DZNep produces maximal Bax translocation to the mitochondria. The results show that EGCG and EGCG/DZNep treatment mobilize Bax to the mitochondria and are consistent with a proapoptotic response to EGCG/DZNep treatment.

DZNep and EGCG deplete PcG proteins and inhibit H3K27 methylation

Previous studies suggest that the PcG genes are key targets of EGCG and DZNep action and that these agents reduce cell survival by

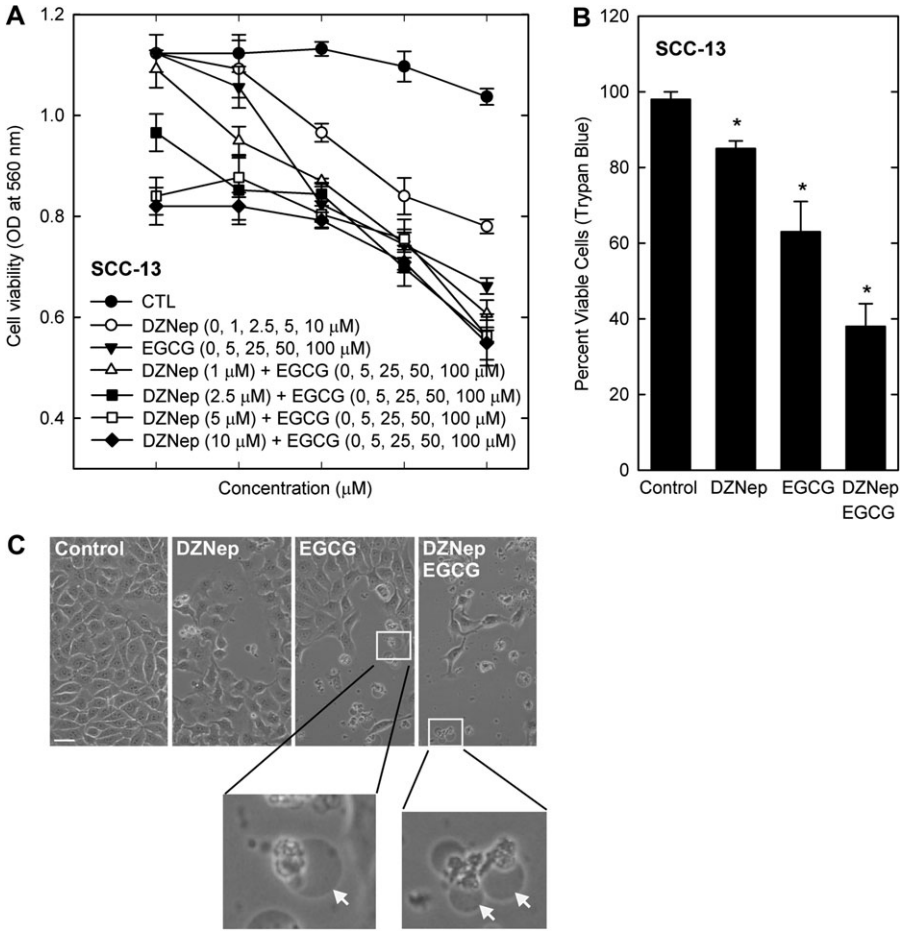

Fig. 1. EGCG and DZNep reduce cell survival. (**A**) SCC-13 cells were treated for 24 h with 1, 2.5, 5 or 10 μM DZNep or 5, 25, 50 or 100 μM EGCG. Parallel groups were treated with 1, 2.5, 5 or 10 μM DZNep in the presence of 0, 5, 25, 50 or 100 μM EGCG for 24 h. The cells were then harvested and viability was assayed by MTT assay. (**B**) DZNep and EGCG reduce SCC-13 cell viability. SCC-13 cells were incubated with 2.5 μM DZNep, 50 μM EGCG or the combination for 24 h and viable cell number was determined by trypan blue assay. The combined treatment produces a >60% reduction in viable cell number. The values are mean ± standard error of the mean, $n = 3$ and the asterisks indicate a significant reduction in cell number compared with control ($P < 0.005$). (**C**) DZNep and EGCG alter SCC-13 cell morphology. SCC-13 cells were treated for 24 h with 2.5 μM DZNep, 50 μM EGCG or 2.5 μM DZNep + 50 μM EGCG and then photographed. The results shown in this figure are representative of four independent experiments. The arrows indicate cell blebs typical of apoptosis (37).

suppressing PcG protein function (14,36). We therefore examined the impact of treatment with EGCG and DZNep on PcG protein level and activity. As shown in Figure 4A, treatment with DZNep or EGCG reduces the level of Ezh2, Eed and Suz12, which are key components of the PRC2 complex. Ezh2 is a histone methyltransferase that catalyzes formation of H3K27me3 (3,39). As shown in Figure 4A, H3K27me3 levels are partially reduced in cells treated with each individual agent and markedly suppressed in cells treated with both agents. We also examined the impact on the PRC1 complex components, Bmi-1 and Ring1B. Ring1B is a histone ubiquitin ligase that catalyzes formation of H2AK119ub (8,40). Ring1B function requires Bmi-1 for optimal activity. Mel18 is a component of the PRC1 complex that can substitute for Bmi-1. We could not detect Ring1B; however, as shown in Figure 4A, Bmi-1 and Mel18 levels are reduced and this is associated with a parallel reduction in H2AK119ub level.

The PcG complex is known to interact with and carry histone deacetylase to the site of PcG interaction with chromatin (41) where HDAC acts to deacetylate histones and thereby help to facilitate formation of closed chromatin (42). Figure 4B shows that HDAC1 level is reduced in DZNep, EGCG and combination treated cells. Moreover, as expected with reduced HDAC1 level, the level of acetylated histone H3 (H3Ac) is increased.

PcG protein loss involves proteasome function

We next examined the mechanism responsible for the reduction in PcG protein level. We chose to monitor regulation of two key PcG proteins, Ezh2 and Bmi-1. We suspected that the reduction may be due to ubiquitination and degradation via the proteasome. To produce a rapid and robust response, we treated cells with elevated (100 μM) EGCG and DZNep (15 μM) concentrations. Figure 5A shows that EGCG treatment causes a marked reduction in Bmi-1 and Ezh2 level and that this suppression is reversed by the proteasome inhibitor, lactacystin. Moreover, staining of total cell extract reveals a general EGCG-dependent increase in ubiquitination (Figure 5B). Immunoprecipitation with anti-Ezh2 or anti-Bmi-1 followed by immunoblot with anti-ubiquitin reveals an increase in Ezh2 and Bmi-1 ubiquitination (Figure 5C). No ubiquitin is detected following immunoprecipitation with anti-IgG, indicating assay specificity. We also examined the impact of DZNep on the level of Bmi-1 and Ezh2. As shown in Figure 5D, Bmi-1 and Ezh2 level are decreased in cells treated with DZNep, EGCG or the combination and this decrease is inhibited by treatment with lactacystin. Thus, DZNep treatment also promotes proteasome-dependent degradation of these targets. In addition, H3K27me3 modification is suppressed by DZNep and this is also reversed by lactacystin (Figure 5D).

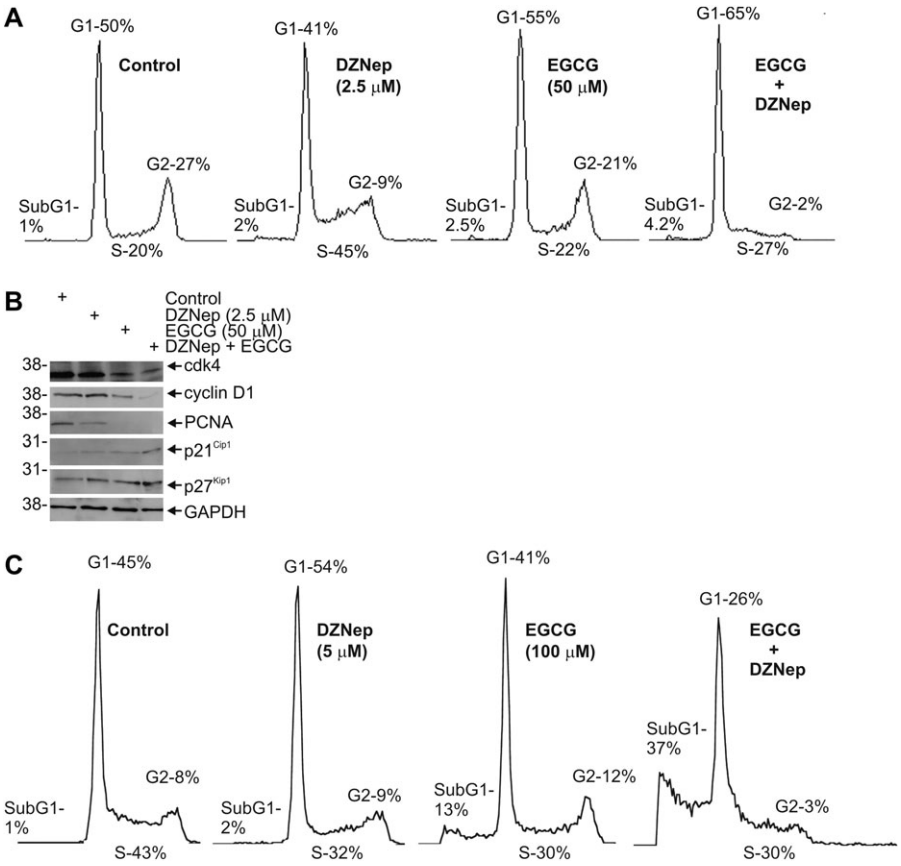

Fig. 2. Cell cycle and cell cycle regulators. SCC-13 cells were treated with 2.5 μM DZNep, 50 μM EGCG or 2.5 μM DZNep + 50 μM EGCG for 24 h. (**A**) Impact on cell cycle. Cell cycle analysis reveals that DZNep treatment causes accumulation of cells in S phase, EGCG produces minimal changes and combination treatment eliminates G_2 and increases subG_1. (**B**) Impact on cell cycle regulatory protein level. SCC-13 cells were treated with DZNep and EGCG in the indicated combinations for 24 h and cell cycle regulatory protein level was monitored by immunoblot. Both compounds alter expression of all markers, but the most profound change is observed when both agents are present. These findings are representative of three independent experiments. (**C**) Impact of elevated DZNep and EGCG levels on cell cycle. SCC-13 cells were treated with the indicated concentrations of DZNep and EGCG for 24 h and cell cycle distribution was monitored. The higher concentrations clearly indicate the tendency of EGCG to produce subG_1 cells and the elevated production of subG_1 cells in EGCG and DZNep-treated cells.

Impact of maintaining Bmi-1 level on EGCG and DZNep-dependent responses

The above studies indicate that DZNep, like EGCG, suppresses PcG protein expression and H3K27me3 formation and that this is associated with reduced cell survival. To assess whether reduced Bmi-1 expression is required for these responses, we infected cells with Bmi-1 encoding adenovirus and then challenged with DZNep or EGCG. As shown in Figure 6A, DZNep or EGCG treatment suppresses Ezh2 level and H3K27me3 formation and this effect is partially reversed by vector-mediated maintenance of Bmi-1 level. Only at the highest EGCG concentration tested (100 μM) did Bmi-1 fail to restore Ezh2 and H3K27me3 level. We next assessed the impact on cell survival. Figure 6B shows that Bmi-1 partially reverses the morphological deterioration observed in DZNep- or EGCG-treated cells and the reduction in cell number (Figure 6C).

Impact of EGCG and DZNep on A431 cells and normal keratinocytes

We next monitored the impact of treatment with EGCG and DZNep on a second skin cancer cell line, A431, and on normal human keratinocytes. A431 cells were treated with 50 μM EGCG, 2.5 μM DZNep or the combination and after 24 h, the cells were harvested and counted. The findings show a reduction in A431 cell number in response to each agent and an additional reduction with both agents. This is associated with a reduction in PcG protein level (Ezh2, Bmi-1) and H3K27me3. In addition, increased apoptotic marker activation (cleaved PARP, cleaved caspase-3) is observed (Figure 7A). In contrast, normal keratinocytes (KERn) are less responsive to treatment (Figure 7B). We observed a trend toward reduced cell number with each agent, but the reduction was not significant. This was associated with a reduction in Ezh2 and Bmi-1 and reduced H3K27me3; however, the reductions were modest compared with that observed in SCC-13 or A431 cells. In addition, accumulation of cleaved PARP and caspase-3 was not observed. Thus, normal keratinocytes appear less responsive to these agents.

Discussion

Targeting polycomb protein function with multiple agents

A host of candidate agents have been described for the prevention of skin cancer and have shown efficacy in a variety of *in vivo* and *in vitro* model systems. However, it is possible that single agent treatment may not be adequate to guarantee long-term prevention of skin cancer. Moreover, the quantity of agent required for prevention may not be achievable due to low solubility, low ability to be absorbed into tissue or rapid clearance. Green tea polyphenol is a promising candidate agent for skin cancer prevention (43–47). However, it may be difficult to achieve adequate levels of the active ingredient, EGCG. These considerations have prompted a search for agents that when given in combination with EGCG enhances uptake or facilitates action (48–50).

The polycomb genes are epigenetic regulators that control chromatin compaction by covalent modification of histones (9,21). The PRC2 complex encodes Ezh2, a methyltransferase that catalyzes

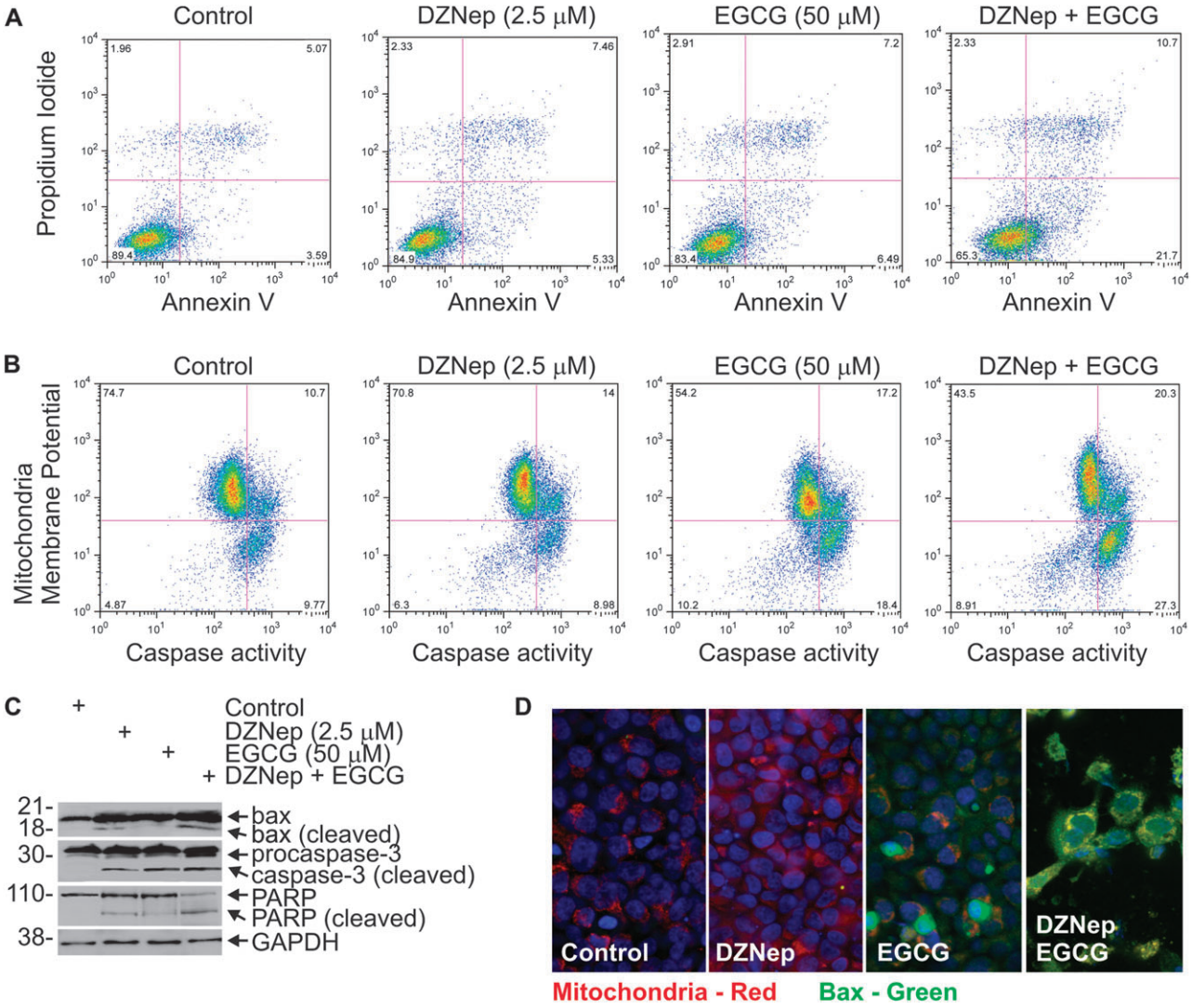

Fig. 3. Impact of EGCG and DZNep on SCC-13 cell apoptosis. SCC-13 cells were treated with 2.5 μM DZNep and 50 μM EGCG as indicated at the top of each panel and at 24 h harvested for cell sorting. (**A**) Annexin V and propidium iodide staining. Results are presented as annexin V (FITC) versus PI fluorescence. Viable cells are PI- and annexin V-negative (bottom left quadrant), PI-negative/annexin V-positive cells are early-apoptotic (bottom right quadrant), PI- and annexin V-positive are late apoptotic (top right quadrant). (**B**) Mitochondria membrane potential and caspase-3/7 activity. Cells were treated as above. Viable cells have high mitochondria membrane potential and low caspase activity (top left quadrant), cells with low mitochondria membrane potential and low caspase activity are cells initiating mitochondria failure early in apoptosis (bottom left quadrant) and cells with low mitochondria membrane potential and high caspase activity are in active apoptosis (lower right quadrant). (**C**) Immunoblot detection of apoptosis markers. Cells were treated as above for 24 h and extracts were prepared for detection of apoptotic markers. (**D**) EGCG/DZNep-treated mitochondria accumulate Bax. Cells were treated as above and during the final 1 h of treatment were incubated with MitoTracker-Red CMXRos for 30 min at 37°C to label mitochondria (red) and then fixed and stained with anti-bax (green). Colocalization of Bax and MitoTracker is indicated in yellow. These findings are representative of four repeated experiments.

H3K27me3 formation, and this complex includes other PcG proteins that interact with Ezh2 to enhance methyltransferase activity (51–53). Ezh2 is known to be overexpressed in skin cancer cells (14). The PRC1 complex encodes Ring1B, Bmi-1, CBX and PH1. Ring1B is an E3 ubiquitin ligase that catalyzes formation of H2AK119ub (8) and Bmi-1 is required for optimal Ring1B activity (8). Previous studies show that EGCG treatment of SCC-13 skin cancer cells reduces the level of Ezh2 and associated proteins (14). EGCG treatment also reduces the level of key PRC1 complex components, including Bmi-1 (14). The reduction in PCR1 and PRC2 component level is associated with increased expression of growth suppressor proteins and reduced expression of pro-proliferation cell cycle regulatory proteins (14). For example, $p21^{Cip1}$ and $p27^{kip1}$ levels are increased and the levels of various cyclins and cdk are reduced and increased apoptosis is observed. Moreover, preventing the EGCG-dependent reduction in Bmi-1 level by vector-mediated expression reverses the EGCG-dependent changes (14).

Impact of treatment with DZNep

In the present study, we examine the impact of cotreatment of skin cancer cells with EGCG and DZNep. DZNep is a potent inhibitor of AdoHcy hydrolase (22–25). Inhibiting AdoHcy hydrolase results in accumulation of AdoHcy, which leads to product inhibition of *S*-adenosyl-L-methionine-dependent methyltransferases and reduces the level of methyl donor groups (24,26). The Ezh2 methyltransferase requires available methyl groups for function and so, we reasoned that limiting methyl group availability may enhance EGCG-dependent activity. We show that treating SCC-13 cells with DZNep reduces PRC2 (Ezh2, Eed, Suz12) and PRC1 (Mel18, Bmi-1) protein level (36). The reduction in Ezh2, Eed and Suz12 is associated with reduced H3K27me3 formation (36), reduced cdk4, cyclin D1 and Proliferating cell nuclear antigen level and increased $p21^{Cip1}$ and $p27^{Kip1}$ levels. Apoptosis is also increased as evidenced by enhanced caspase-3, PARP and bax cleavage and mobilization of cleaved bax to the

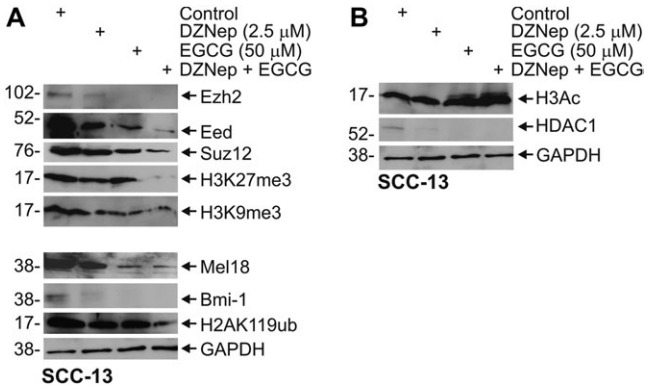

Fig. 4. Impact of EGCG and DZNep on PcG protein and HDAC level. (**A** and **B**) EGCG and DZNep suppress PcG protein level. SCC-13 cells were treated with the indicated agent for 24 h and total cell extracts were prepared for immunoblot detection of the indicated targets. Similar changes were observed in each of five independent experiments.

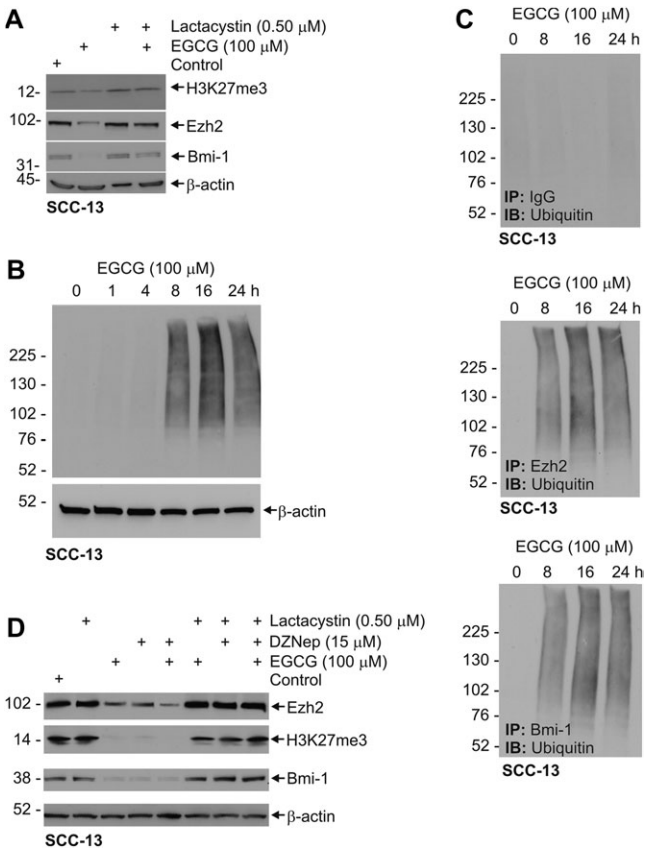

Fig. 5. Loss of Bmi-1 and Ezh2 requires proteasome function. SCC-13 cells were plated at subconfluent density and permitted to attach. After 24 h, the cells were treated for an additional 24 h with the indicated concentrations of lactacystin, EGCG, DZNep or a combination of these agents. (**A**) SCC-13 cells were treated as above and then extracts were prepared for detection of each indicated protein. (**B**) Impact of EGCG on overall level of ubiquitination. Cells were treated for 0–24 h with 100 μM EGCG and total extracts were prepared for immunoblot with anti-ubiquitin. Loading was normalized to the level of β-actin. (**C**) SCC-13 cells were treated as above (panel B) and total extracts were immunoprecipitated with the indicated antibodies. The precipitates were then electrophoresed and immunoblotted to detect ubiquitin. The normal mouse anti-IgG is from Santa Cruz Biotecnology Inc (sc-2025). (**D**) SCC-13 cells were treated as above (panel A) and extracts were prepared and electrophoresed for immunoblot to detect the indicated proteins. Similar results were observed in each of three independent repeated experiments.

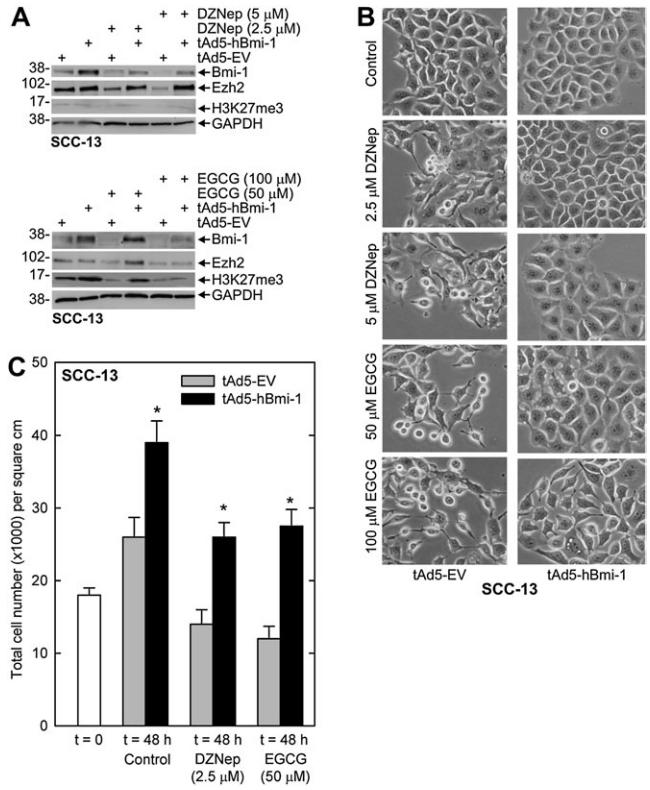

Fig. 6. Impact of maintenance of Bmi-1 expression on SCC-13 cell response to DZNep and EGCG. (**A**) SCC-13 cells (8×10^4 per well) were seeded in 35 mm dishes and permitted to attach overnight. The cells were then incubated with empty or Bmi-1 encoding adenovirus and after 24 h treated for an additional 24 h with the indicated agent. Extracts were then prepared for immunoblot detection of the indicated epitopes. (**B** and **C**) After treatment as indicated above, the cells were photographed and then harvested and counted. The values are mean ± standard error of the mean, $n = 3$, and asterisks indicate tAd5-hBmi-1 values significantly higher ($P < 0.005$) than the paired tAd5-EV control value using Student's *t*-test.

mitochondria. These results are consistent with observations in acute myeloid leukemia and breast cancer cells. DZNep treatment of acute myeloid leukemia cells reduces Ezh2 level and H3K27me3 formation, reduces cyclin E level, increases p16, $p21^{Cip1}$ and $p27^{Kip1}$ level and promotes apoptosis (36). In breast cancer, DZNep reduces Ezh2, Eed and Suz12 level and H3K27me3 formation and induces apoptosis (28). DZNep is also active in other systems. DZNep treatment of multiple myeloma cells with restores expression of polycomb-suppressed genes and reduces tumor load (30). DZNep also alters PcG target gene expression in NK cells (31), reduces Ezh2 level in breast cancer cells (32), impairs glioblastoma cancer stem cell renewal *in vitro* and *in vivo* (34) and reduces mammary tumor cell survival (35). Thus, our findings are consistent with observations in these other cell types. Moreover, we observe similar effects in a second skin cancer cell line, A431, suggesting that this is a general response to treating skin cancer cells with these agents. In contrast, normal human keratinocytes appear to be more resistant to the impact of EGCG and DZNep, as the reduction in PcG gene expression and H3K27me3 formation are less pronounced and apoptosis is minimal. This may suggest that these agents may be useful in treating tumor cells and not impact normal cells.

The EGCG and DZNep-dependent reduction in PcG protein is proteasome dependent

The intracellular mechanism of PcG protein suppression by DZNep is not well understood. Direct inhibition of Ezh2 methyltransferase activity appears unlikely, as DZNep is an AdoHcy hydrolase inhibitor

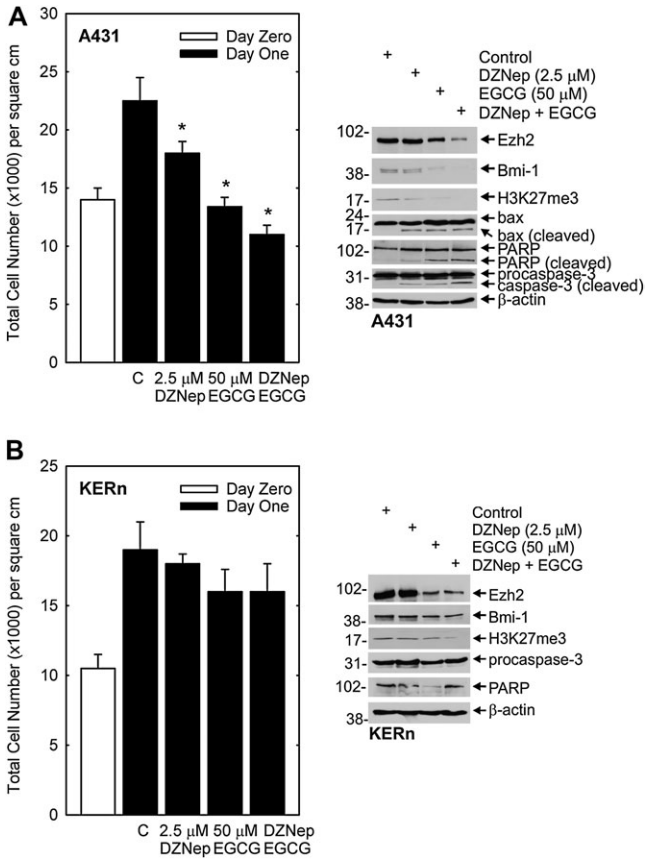

Fig. 7. Impact of EGCG and DZNep on A431 cells and normal keratinocytes. (**A** and **B**) A431 cells or normal keratinocytes (KERn) were treated with 2.5 μM DZNep, 50 μM EGCG or the combination for 24 h and then harvested for cell counting and preparation of extracts for immunoblot. The graph values are mean number of cells per square centimeters ± standard error of the mean, $n = 3$. The asterisks indicate a statistically significant reduction in cell number as compared with Day 1 untreated control cells (**C**) as determined using the Student's *t*-test ($P < 0.005$).

(22–25). Inhibition of AdoHcy limits methyl donor availability. Thus, it is probable that inhibition of Ezh2 activity is due to a lack of available methyl groups. However, this interpretation is complicated by the fact that DZNep treatment in SCC-13 cells reduces Ezh2 level (29,30,32,54,55), suggesting that the impact of not strictly inhibition of activity. The major impact is the reduction in Ezh2 level and a key question is the mechanism of this reduction. In the present study, we show that treatment with the proteasome inhibitor, lactacystin, inhibits the DZNep-dependent Ezh2 reduction. This DZNep-dependent reduction in Ezh2 level is associated with reduced H3K27me3 formation, which is an Ezh2-specific histone modification. This finding is consistent with one other report showing that DZNep promotes proteasome-dependent Ezh2 degradation (36). It is also of interest that DZNep treatment reduces expression of other PcG proteins. Additional studies will be required to understand this regulation, but it is possible that destabilizing a subset of PcG proteins in the PRC2 or PRC1 complex changes the conformation of the other components such that they are also targeted for degradation. It is of particular interest that DZNep treatment triggers proteasome-dependent degradation of Bmi-1, a PRC1 complex protein. This suggests that perturbing methyl donor availability produces broad changes in PcG function. It may be that Bmi-1 levels are reduced due to an indirect effect of Ezh2 suppression, which leads to reduction in H3K27me3. Since H3K27me3 is the Bmi-1 chromatin-binding site, its reduced level may destabilize Bmi-1.

EGCG treatment also reduces Mel18, Ezh2, eed, Suz12 and Bmi-1 level. Mechanistic studies show that EGCG treatment increases Ezh2 and Bmi-1 ubiquitination and that this is associated with loss of these proteins. The proteasome appears to have a role, as the loss is prevented by lactacystin. An interesting feature is that DZNep and EGCG increase H3Ac formation. This is remarkable, considering that EGCG functions as a histone acetyltransferase inhibitor in some systems (56). This does not appear to be the case in SCC-13 cells (15,20). Our present studies suggest that H3Ac increase is due to reduced HDAC expression.

H3K27me3 and histone H3 trimethylated on lysine 9

We show that EGCG and DZNep treatment is associated with reduced H3K27me3 formation. The loss of these marks is associated with 'open chromatin' (57). Although we observe a substantial reduction in H3K27me3 formation in DZNep and EGCG-treated cells, there was no reliable change in histone H3 trimethylated on lysine 9 formation. Thus, DZNep and EGCG do not trigger changes in all marks associated with open chromatin. We show that treatment with EGCG or DZNep suppresses HDAC1 level leading to increased H3Ac formation. Although it is known that histone deacetylase associates with PcG proteins and HDAC inhibitors, we do not know if the reduction in HDAC1 level is an indirect effect due to changes in PcG level or a direct effect on HDAC1 transcription or stability. In addition, HDAC inhibitors have been shown to suppress PcG protein level (58–62). Thus, the relationship among these epigenetic regulators is complex.

In summary, our studies show that cotreatment with EGCG and DZNep is more effective than treatment with either individual agent, suggesting that coadministration of these agents may enhance chemopreventive efficiency in skin cancer. Although EGCG is known to be readily tolerated without side effects, the impact of repeated administration of DZNep is not presently known. However, it does appear to suppress tumor growth in mice (35,54). These studies suggest that targeting methyl donor availability along with antioxidant treatment is more efficient than either treatment alone.

Funding

National Institutes of Health (AR053851 and CA131074 to R.L.E.).

Conflict of Interest Statement: None declared.

References

1. Orlando,V. (2003) Polycomb, epigenomes, and control of cell identity. *Cell*, **112**, 599–606.
2. Valk-Lingbeek,M.E. *et al*. (2004) Stem cells and cancer; the polycomb connection. *Cell*, **118**, 409–418.
3. Simon,J.A. *et al*. (2008) Roles of the EZH2 histone methyltransferase in cancer epigenetics. *Mutat. Res.*, **647**, 21–29.
4. Pasini,D. *et al*. (2004) Suz12 is essential for mouse development and for EZH2 histone methyltransferase activity. *EMBO J.*, **23**, 4061–4071.
5. Cao,R. *et al*. (2004) SUZ12 is required for both the histone methyltransferase activity and the silencing function of the EED-EZH2 complex. *Mol. Cell.*, **15**, 57–67.
6. Simon,J.A. *et al*. (2009) Mechanisms of polycomb gene silencing: knowns and unknowns. *Nat. Rev. Mol. Cell Biol.*, **10**, 697–708.
7. Hatano,A. *et al*. (2010) Phosphorylation of the chromodomain changes the binding specificity of Cbx2 for methylated histone H3. *Biochem. Biophys. Res. Commun.*, **397**, 93–99.
8. Li,Z. *et al*. (2006) Structure of a Bmi-1-Ring1B polycomb group ubiquitin ligase complex. *J. Biol. Chem.*, **281**, 20643–20649.
9. Levine,S.S. *et al*. (2004) Division of labor in polycomb group repression. *Trends Biochem. Sci.*, **29**, 478–485.
10. Sparmann,A. *et al*. (2006) Polycomb silencers control cell fate, development and cancer. *Nat. Rev. Cancer.*, **6**, 846–856.
11. Fischle,W. *et al*. (2003) Molecular basis for the discrimination of repressive methyl-lysine marks in histone H3 by Polycomb and HP1 chromodomains. *Genes Dev.*, **17**, 1870–1881.
12. Cao,R. *et al*. (2005) Role of Bmi-1 and Ring1A in H2A ubiquitylation and Hox gene silencing. *Mol. Cell.*, **20**, 845–854.

13. Jacobs,J.J. *et al*. (2002) Polycomb repression: from cellular memory to cellular proliferation and cancer. *Biochim. Biophys. Acta.*, **1602**, 151–161.
14. Balasubramanian,S. *et al*. (2010) The Bmi-1 polycomb protein antagonizes the (-)-epigallocatechin-3-gallate-dependent suppression of skin cancer cell survival. *Carcinogenesis*, **31**, 496–503.
15. Balasubramanian,S. *et al*. (2008) The Bmi-1 polycomb group gene in skin cancer: regulation of function by (-)-epigallocatechin-3-gallate. *Nutr. Rev.*, **66** (suppl. 1), S65–S68.
16. Nihal,M. *et al*. (2005) Anti-proliferative and proapoptotic effects of (-)-epigallocatechin-3-gallate on human melanoma: possible implications for the chemoprevention of melanoma. *Int. J. Cancer.*, **114**, 513–521.
17. Gupta,S. *et al*. (2002) Green tea and prostate cancer. *Urol. Clin. North Am.*, **29**, 49–57, viii.
18. Katiyar,S.K. *et al*. (2001) Green tea polyphenol (-)-epigallocatechin-3-gallate treatment to mouse skin prevents UVB-induced infiltration of leukocytes, depletion of antigen-presenting cells, and oxidative stress. *J. Leukoc. Biol.*, **69**, 719–726.
19. Mukhtar,H. *et al*. (2000) Tea polyphenols: prevention of cancer and optimizing health. *Am. J. Clin. Nutr.*, **71**, 1698S–1702S.
20. Lee,K. *et al*. (2008) Expression of Bmi-1 in epidermis enhances cell survival by altering cell cycle regulatory protein expression and inhibiting apoptosis. *J. Invest. Dermatol.*, **128**, 9–17.
21. Lund,A.H. *et al*. (2004) Polycomb complexes and silencing mechanisms. *Curr.Opin. Cell Biol.*, **16**, 239–246.
22. Glazer,R.I. *et al*. (1986) 3-Deazaneplanocin: a new and potent inhibitor of S-adenosylhomocysteine hydrolase and its effects on human promyelocytic leukemia cell line HL-60. *Biochem. Biophys. Res. Commun.*, **135**, 688–694.
23. Glazer,R.I. *et al*. (1986) 3-Deazaneplanocin A: a new inhibitor of S-adenosylhomocysteine synthesis and its effects in human colon carcinoma cells. *Biochem. Pharmacol.*, **35**, 4523–4527.
24. Chiang,P.K. *et al*. (1979) Perturbation of biochemical transmethylations by 3-deazaadenosine in vivo. *Biochem. Pharmacol.*, **28**, 1897–1902.
25. Liu,S. *et al*. (1992) Rational approaches to the design of antiviral agents based on S-adenosyl-L-homocysteine hydrolase as a molecular target. *Antiviral Res.*, **19**, 247–265.
26. Chiang,P.K. *et al*. (1992) Activation of collagen IV gene expression in F9 teratocarcinoma cells by 3-deazaadenosine analogs. Indirect inhibitors of methylation. *J. Biol. Chem.*, **267**, 4988–4991.
27. Chiang,P.K. (1981) Conversion of 3T3-L1 fibroblasts to fat cells by an inhibitor of methylation: effect of 3-deazaadenosine. *Science*, **211**, 1164–1166.
28. Tan,J. *et al*. (2007) Pharmacologic disruption of Polycomb-repressive complex 2-mediated gene repression selectively induces apoptosis in cancer cells. *Genes Dev.*, **21**, 1050–1063.
29. Toth,Z. *et al*. (2010) Epigenetic analysis of KSHV latent and lytic genomes. *PLoS Pathog.*, **6**, e1001013.
30. Kalushkova,A. *et al*. (2010) Polycomb target genes are silenced in multiple myeloma. *PLoS One*, **5**, e11483.
31. Nagel,S. *et al*. (2010) Polycomb repressor complex 2 regulates HOXA9 and HOXA10, activating ID2 in NK/T-cell lines. *Mol. Cancer.*, **9**, 151.
32. Hayden,A. *et al*. (2011) S-adenosylhomocysteine hydrolase inhibition by 3-deazaneplanocin A analogues induces anti-cancer effects in breast cancer cell lines and synergy with both histone deacetylase and HER2 inhibition. *Breast Cancer Res. Treat.*, **107**, 109–119.
33. Musch,T. *et al*. (2010) Nucleoside drugs induce cellular differentiation by caspase-dependent degradation of stem cell factors. *PLoS One*, **5**, e10726.
34. Suva,M.L. *et al*. (2009) EZH2 is essential for glioblastoma cancer stem cell maintenance. *Cancer Res.*, **69**, 9211–9218.
35. Puppe,J. *et al*. (2009) BRCA1-deficient mammary tumor cells are dependent on EZH2 expression and sensitive to Polycomb Repressive Complex 2-inhibitor 3-deazaneplanocin A. *Breast Cancer Res.*, **11**, R63.
36. Fiskus,W. *et al*. (2009) Combined epigenetic therapy with the histone methyltransferase EZH2 inhibitor 3-deazaneplanocin A and the histone deacetylase inhibitor panobinostat against human AML cells. *Blood*, **114**, 2733–2743.
37. Efimova,T. *et al*. (2004) Protein kinase Cdelta regulates keratinocyte death and survival by regulating activity and subcellular localization of a p38delta-extracellular signal-regulated kinase 1/2 complex. *Mol. Cell. Biol.*, **24**, 8167–8183.
38. Chou,T.C. (2006) Theoretical basis, experimental design, and computerized simulation of synergism and antagonism in drug combination studies. *Pharmacol. Rev.*, **58**, 621–681.
39. Cao,R. *et al*. (2004) The functions of E(Z)/EZH2-mediated methylation of lysine 27 in histone H3. *Curr. Opin. Genet. Dev.*, **14**, 155–164.
40. de Bie,P. *et al*. (2010) Regulation. of the polycomb protein RING1B ubiquitination by USP7. *Biochem. Biophys. Res. Commun.*, **400**, 389–395.
41. van der Vlag,J. *et al*. (1999) Transcriptional repression mediated by the human polycomb-group protein EED involves histone deacetylation. *Nat. Genet.*, **23**, 474–478.
42. Bolden,J.E. *et al*. (2006) Anticancer activities of histone deacetylase inhibitors. *Nat. Rev. Drug Discov.*, **5**, 769–784.
43. Khan,N. *et al*. (2006) Targeting multiple signaling pathways by green tea polyphenol (-)-epigallocatechin-3-gallate. *Cancer Res.*, **66**, 2500–2505.
44. Katiyar,S.K. *et al*. (1993) Protection against malignant conversion of chemically induced benign skin papillomas to squamous cell carcinomas in SENCAR mice by a polyphenolic fraction isolated from green tea. *Cancer Res.*, **53**, 5409–5412.
45. Agarwal,R. *et al*. (1993) Protection against ultraviolet B radiation-induced effects in the skin of SKH-1 hairless mice by a polyphenolic fraction isolated from green tea. *Photochem. Photobiol.*, **58**, 695–700.
46. Park,A.M. *et al*. (2003) Signal transduction pathways: targets for green and black tea polyphenols. *J. Biochem. Mol. Biol.*, **36**, 66–77.
47. Chung,J.Y. *et al*. (1999) Inhibition of activator protein 1 activity and cell growth by purified green tea and black tea polyphenols in H-ras-transformed cells: structure-activity relationship and mechanisms involved. *Cancer Res.*, **59**, 4610–4617.
48. Lambert,J.D. *et al*. (2008) Effect of genistein on the bioavailability and intestinal cancer chemopreventive activity of (-)-epigallocatechin-3-gallate. *Carcinogenesis*, **29**, 2019–2024.
49. Suganuma,M. *et al*. (2006) Green tea polyphenol stimulates cancer preventive effects of celecoxib in human lung cancer cells by upregulation of GADD153 gene. *Int. J. Cancer.*, **119**, 33–40.
50. Lambert,J.D. *et al*. (2004) Piperine enhances the bioavailability of the tea polyphenol (-)-epigallocatechin-3-gallate in mice. *J. Nutr.*, **134**, 1948–1952.
51. Sarma,K. *et al*. (2008) Ezh2 requires PHF1 to efficiently catalyze H3 lysine 27 trimethylation *in vivo*. *Mol. Cell. Biol.*, **28**, 2718–2731.
52. Kuzmichev,A. *et al*. (2005) Composition and histone substrates of polycomb repressive group complexes change during cellular differentiation. *Proc. Natl Acad. Sci. USA.*, **102**, 1859–1864.
53. Kuzmichev,A. *et al*. (2002) Histone methyltransferase activity associated with a human multiprotein complex containing the enhancer of Zeste protein. *Genes Dev.*, **16**, 2893–2905.
54. Smits,M. *et al*. (2010) miR-101 is down-regulated in glioblastoma resulting in EZH2-induced proliferation, migration, and angiogenesis. *Oncotarget*, **1**, 710–720.
55. Smits,M. *et al*. (2011) Down-regulation of miR-101 in endothelial cells promotes blood vessel formation through reduced repression of EZH2. *PLoS One*, **6**, e16282.
56. Choi,K.C. *et al*. (2009) Epigallocatechin-3-gallate, a histone acetyltransferase inhibitor, inhibits EBV-induced B lymphocyte transformation via suppression of RelA acetylation. *Cancer Res.*, **69**, 583–592.
57. Perry,A.S. *et al*. (2010) The epigenome as a therapeutic target in prostate cancer. *Nat. Rev. Urol.*, **7**, 668–680.
58. Grant,S. (2010) HDAC inhibitors repress the polycomb protein BMI1. *Cell Cycle*, **9**, 2705–2706.
59. Yaswen,P. (2010) HDAC inhibitors conquer Polycomb proteins. *Cell Cycle*, **9**, 2705.
60. Bommi,P.V. *et al*. (2010) The. polycomb group protein BMI1 is a transcriptional target of HDAC inhibitors. *Cell Cycle*, **9**, 2663–2673.
61. Yamaguchi,J. *et al*. (2010) Histone deacetylase inhibitor (SAHA) and repression of EZH2 synergistically inhibit proliferation of gallbladder carcinoma. *Cancer Sci.*, **101**, 355–362.
62. Jung,J.W. *et al*. (2010) Histone deacetylase controls adult stem cell aging by balancing the expression of polycomb genes and jumonji domain containing 3. *Cell. Mol. Life Sci.*, **67**, 1165–1176.

Received April 13, 2011; revised June 28, 2011; accepted July 15, 2011